Polymorphism in 4′-Hydroxyacetophenone: Structure and Energetics

ARTICLE *in* CRYSTAL GROWTH & DESIGN · JUNE 2008

Impact Factor: 4.89 · DOI: 10.1021/cg7012792

CRYSTAL GROWTH & DESIGN
2008
VOL. 8, NO. 7
2419–2430

Polymorphism in 4′-Hydroxyacetophenone: Structure and Energetics

Carlos E. S. Bernardes,[†] M. Fátima M. Piedade,[†,‡] and Manuel E. Minas da Piedade*[,†]

Departamento de Química e Bioquímica, Faculdade de Ciências, Universidade de Lisboa, 1649-016 Lisboa, Portugal, and Centro de Química Estrutural, Complexo Interdisciplinar, Instituto Superior Técnico da Universidade Técnica de Lisboa, 1049-001 Lisboa, Portugal

Received December 31, 2007; Revised Manuscript Received February 25, 2008

ABSTRACT: A new polymorph of 4′-hydroxyacetophenone (form I, monoclinic, $P2_1/c$, $Z' = 1$) was isolated and characterized. The structural differences between this phase and the previously known one (form II, orthorhombic, $P2_12_12_1$, $Z' = 2$) were investigated by X-ray diffraction. The two polymorphs exhibit distinct packing features and, at the molecular level, they seem to differ by the relative conformations of the OH and $C(O)CH_3$ groups. The stability domains of the two phases from 298.15 K to the fusion temperature were also studied by a variety of thermodynamic methods and by density functional theory calculations. On the basis of the obtained results, $p-T$ and $\Delta_f G^o_m - T$ phase diagrams for 4′-hydroxyacetophenone were defined. Differential scanning calorimetry experiments indicated that the system is enantiotropic, with form II first transforming into form I at 351.2 ± 2.7 K, followed by fusion of form I at 381.9 ± 0.1 K. Solution calorimetry demonstrated that form II is more stable than form I at 298.15 K, with $\Delta_{trs}H^o_m(II \rightarrow I) = 0.49 \pm 0.13$ kJ mol^{-1}. Despite this small enthalpy difference compared to the thermal energy at 298.15 K (RT = 2.5 kJ mol^{-1}), a sample of form I could be stored at ambient temperature, for at least 1 year, without change. Results of B3LYP/6–31G(d,p) calculations indicated that the most stable conformation of the isolated molecule is also that corresponding to the most stable polymorph of 4′-hydroxyacetophenone at ambient temperature (form II). The computations further suggest that the occurrence of the II → I transition through a simple rotation of the OH group is unlikely. Finally, the fact that the more stable form II has a greater Z' than the less stable form I contrasts with the recent proposal that high Z' polymorphs are metastable precursors of lower Z' forms along the crystallization pathway.

Introduction

Since the middle of the last century, it has been widely recognized that many organic compounds can be obtained in more than one crystal structure, a phenomenon known as polymorphism.[1,2] It also became apparent that the adopted crystal structure often exerts a significant effect in the solid-state properties of the compounds, so that in fact, each polymorph should be regarded as a different material. Hence, the control of polymorphism provides a means to tune the properties of a product in view of an application, without changing the molecule involved. The achievement of this goal currently has a strong impact in the production, shelf life, and patenting of organic conductors, pigments, or pharmaceuticals.[1,2] From a more fundamental point of view, polymorphism is also an important phenomenon to probe the mechanisms of crystallization and the intermolecular interactions that determine the molecular arrangements in the crystal structures.[1–4]

Organic polymorphs can often coexist at the same temperature, but they may evolve over time to the most thermodynamically stable one. Therefore, once polymorphism is identified, it is very important to define a stability hierarchy among different forms. In most applications, the compounds are used at ambient temperature and pressure. Typical ambient pressure changes (even when the samples are subject to vacuum-drying operations) are usually not sufficient to induce phase transitions. The same is not true, however, for ambient temperature, which can undergo significant variations between winter and summer, in various zones of the globe. Therefore, it is normally desirable to establish the stability domains of the various forms at ambient pressure (or below) and in a range as large as possible around 298 K. To this end, one is frequently interested in three questions: (i) Are the polymorphs monotropically (i.e., one is more stable than the other at any temperature before fusion) or enantiotropically related (i.e., there is a transition temperature before fusion at which the stability order is reversed)? (ii) For an enantiotropic system, what is the transition temperature, T_{trs}? (iii) What are the pressure vs temperature or Gibbs energy vs temperature diagrams that define the location of the phase boundaries for the substance under examination? These questions are most conveniently addressed within the scope of thermodynamics.[5–11]

4′-Hydroxyacetophenone (HAP) is a versatile compound with significant commercial applications and additional potential end-uses. These include rubber and plastics, pharmaceuticals, agricultural chemicals, flavor and fragrances, and cosmetics. To date, only an orthorhombic form, which we now dub form II, was known.[12–14] Here, we describe the isolation of a new polymorph of 4′-hydroxyacetophenone (form I, monoclinic) that can be prepared in a reproducible way and stored at room temperature for long periods of time without apparent decomposition. The nature of the structural differences between forms I and II was investigated by X-ray diffraction and computational chemistry methods, and their stability domains were characterized by several thermodynamic techniques.

Materials and Methods

General. The ^{1}H NMR spectra were obtained in $CDCl_3$, at ambient temperature, on a Bruker Ultrashield 400 MHz spectrometer. GC-MS experiments were performed on an Agilent 6890 gas chromatograph coupled to an Agilent 5973*N* mass detector. A TRB-5MS capillary column from Teknokroma (5% diphenyl/95% dimethylpolysiloxane; 30 m × 0.25 mm I.D., 0.25 μm d_f) was used. The carrier gas was helium maintained at a constant pressure of 1.19 bar. A vaporization injector operating in the split mode (1:100), at 523 K, was employed, and the oven temperature was programmed as follows: 323 K (1 min),

* Corresponding author. E-mail: memp@fc.ul.pt.
† Universidade de Lisboa.
‡ Instituto Superior Técnico da Universidade Técnica de Lisboa.

10.1021/cg7012792 CCC: $40.75
Published on Web 06/17/2008

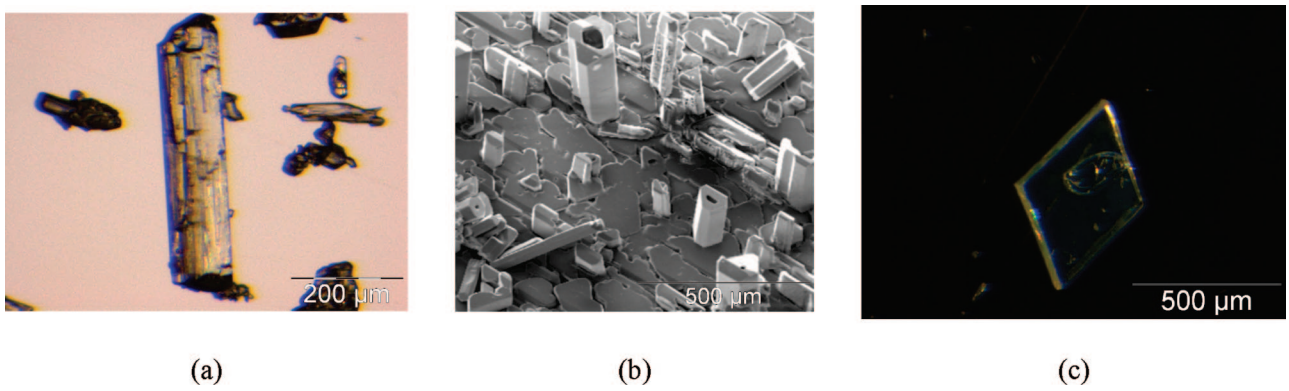

Figure 1. (a) Optical microscopy image of monoclinic crystals of 4′-hydroxyacetophenone (form I) prepared by heating the sublimed HAP starting material in an oven at 363 K. (b) SEM image of tubular shaped crystals of form I. (c) Optical microscopy image of an orthorhombic crystal of 4′-hydroxyacetophenone (form II).

ramp at 10 K min^{-1}, 523 K (10 min). The transfer line, ion source, and quadrupole analyzer were maintained at 553, 503, and 423 K, respectively, and a solvent delay of 5 min was selected. In the full-scan mode, electron ionization mass spectra in the range 35–550 Da were recorded at 70 eV electron energy and with an ionization current of 34.6 μA. Data recording and instrument control were performed by the MSD ChemStation software from Agilent (G1701CA; version C.00.00). The identity of the analyzed compound was assigned by comparison of the mass-spectrometric results with the data in Wiley's reference spectral databank (G1035B, Rev D.02.00) and its purity was calculated from the normalized peak areas, without using correction factors to establish abundances. The X-ray powder diffractograms were recorded on a Philips PW1730 diffractometer, with automatic data acquisition (APD Philips v.35B), operating in the $\theta-2\theta$ mode. The apparatus had a vertical goniometer (PW1820), a proportional xenon detector (PW1711), and a graphite monocromator (PW1752). A Cu Kα radiation source was used. The tube amperage was 30 mA and the tube voltage 40 kV. The diffractograms were recorded in the range $10° \leq 2\theta \leq 35°$, in the continuous mode, with a step size of 0.015°(2θ), and an acquisition time of 1.5 s/step. The samples were mounted on an aluminum sample holder. The indexation of the powder patterns was performed using the program Checkcell.[15] Optical microscopy images were obtained with an Olympus SZX10 stereoscopic microscope and the Cell^D 2.6 software. Scanning Electron Microscopy (SEM) images on Au/Pd-sputtered samples were performed in high vacuum, using a FEI Quanta 400 ESEM apparatus, with a resolution of 2 nm. The electron beam voltage was set to 10 kV.

Ethanol (Merck, p.a.) used in the crystallization and in the solution calorimetry experiments was dried over small slices of sodium and distilled under nitrogen atmosphere. Distilled and deionized water from a Millipore system (conductivity $\leq$0.1 μS) was used in the preparation of all aqueous solutions. The 4′-hydroxyacetophenone (HAP, 98% Aldrich) used as starting material for the synthesis of the polymorphic forms was purified by sublimation at 368 K and 13 Pa. ^{1}H NMR (400 MHz, $CDCl_3$/TMS): 7.91 (d, CH, 2H), 6.92 (d, CH, 2H), 2.58 (s, CH_3, 3H). These results are in accordance with those published in a reference database.[16] No impurities were detected by GC-MS.

Synthesis of Monoclinic HAP (Form I). Crystals of the monoclinic form I (Figure 1a) were obtained by heating the sublimed HAP starting material in an oven, at 363 K, under nitrogen atmosphere (ca. 1 bar), during six days. The powder pattern was indexed as monoclinic, space group $P2_1/c$, with $a = 7.707(2)$ Å, $b = 8.335(3)$ Å, $c = 11.282(3)$ Å, $\beta = 95.10(2)°$. Monoclinic crystals of form I with a tubular morphology (Figure 1b) were also prepared as follows. A suspension of 1.7 g of HAP in 30 g of water was kept at 338 K, under magnetic stirring, inside a 50 cm^3 beaker, until complete dissolution of the solid was observed. The solution was allowed to cool to room temperature (ca. 298 K), without stirring or control of the cooling rate, and maintained at this temperature for ca. 24 h. Large tubular crystals of the monoclinic form I were selected from the precipitated material, transferred to a filter paper to remove most of the water, and dried in air at 298 $\pm$ 2 K for 2 weeks. The powder pattern of the dried crystals was indexed as monoclinic, space group $P2_1/c$, with $a = 7.744(10)$ Å, $b = 8.330(10)$ Å, $c = 11.289(10)$ Å, $\beta = 94.92(11)°$. The unit cell dimensions obtained from the indexation of the powder patterns corresponding to the monoclinic HAP crystals with the different morphologies shown in images a and b in Figure 1 are consistent with those obtained in this work by single-crystal X-ray diffraction at 298 K: $a = 7.7200(15)$ Å, $b = 8.3600(17)$ Å, $c = 11.280(2)$ Å, and $\beta = 95.02(3)°$ (see below). Samples of form I stored in air at room temperature for more than 1 year showed no evidence of undergoing a phase transition to form II, when analyzed by X-ray powder diffraction.

Synthesis of Orthorhombic HAP (Form II). A suspension of HAP in dried ethanol was prepared inside a Schlenk tube, under a nitrogen atmosphere, at 323 K. The mixture was kept under magnetic stirring for 2 hours and then heated to 333 K until complete dissolution of the solid was achieved. The resulting solution was maintained at this temperature for 1 h and then cooled to 277 K, without stirring, at a rate of 0.01 K min^{-1}. The precipitated crystals (Figure 1c), were separated from the mother liquor by filtration, washed with cold dry ethanol, and dried in air at 298 $\pm$ 2 K for 2 weeks. The powder pattern was indexed as orthorhombic, space group $P2_12_12_1$, with $a = 6.139(2)$ Å, $b = 9.564(3)$ Å, $c = 24.411(7)$ Å. These values are very similar to those obtained from single crystal X-ray diffraction experiments carried out at room temperature, in this work, $a = 6.1097(11)$ Å, $b = 9.5293(14)$ Å, $c = 24.313(4)$ Å (see below), and previously reported, $a = 6.132(2)$ Å, $b = 9.541(2)$ Å, $c = 24.34(3)$ Å.[13]

Crystal Structure Determination. Single-crystal X-ray diffraction analysis of forms I and II of HAP was performed on a Bruker AXS APEX CCD area detector diffractometer, using graphite-monochromated Mo Kα ($\lambda = 0.710\ 73$ Å) radiation. Intensities were corrected for Lorentz polarization effects. An empirical absorption correction was applied using SADABS[17] and the data reduction was done with the SMART and SAINT programs.[18] All structures were solved by direct methods with SIR97[19] and refined by full-matrix least-squares on F^2 using SHELXL97,[20] both included in WINGX, version 1.70.01.[21] Non-hydrogen atoms were refined with anisotropic thermal parameters. All hydrogen atoms were located in a Fourier map and their positions and isotropic displacement parameters, U_{iso}(H), refined freely, except for those of the methyl group in the structures determined at 298 K. These where placed in idealized positions and constrained to ride on their parent atoms, with C−H distances of 0.96 Å and with U_{iso}(H) values set to 1.5U_{eq}(methyl C). Graphical representations were prepared using Raster3D[22] and Mercury 1.1.2.[23] The intermolecular interactions were calculated with the PARST program.[24] A summary of the crystal data, structure solution, and refinement parameters obtained at 298 and 150 K is given in Table 1.

Differential Scanning Calorimetry (DSC). The DSC studies of the monoclinic and orthorhombic forms of HAP were made in a Setaram TG-DSC 111. The experiments were carried out under a flow of nitrogen of 10 cm^3 min^{-1}. The samples, with masses in the range 5−20 mg, were sealed in aluminum crucibles and heated from 298 to 393 K at a scan rate of 1 K min^{-1}.

Combustion Calorimetry. The standard energy of combustion of monoclinic HAP (form I) was measured by microcombustion calorimetry. Details of the apparatus and the general experimental procedure have been reported.[25,26] In a typical experiment a pellet of the compound (19−32 mg) was placed in a platinum crucible and weighed

Table 1. Crystal Data and Structure Refinement Parameters for Forms I and II of 4′-Hydroxyacetophenone at 298 and 150 K

	form I	form I	form II	form II
empirical formula	C8H8O2	C8H8O2	C8H8O2	C8H8O2
fw	136.15	136.15	136.15	136.15
T (K)	298(2)	150(2)	298(2)	150(1)
wavelength (Å)	0.71073	0.71073	0.71073	0.71073
cryst size (mm^3)	0.19 × 0.09 × 0.06	0.20 × 0.20 × 0.10	0.15 × 0.12 × 0.07	0.5 × 0.15 × 0.08
color of crystal	colorless	colorless	colorless	colorless
cryst syst	monoclinic	monoclinic	orthorhombic	orthorhombic
space group	$P2_{1/c}$	$P2_{1/c}$	$P2_12_12_1$	$P2_12_12_1$
a (Å)	7.7200(15)	7.538(2)	6.1097(11)	6.1554(17)
b (Å)	8.3600(17)	8.380(2)	9.5293(14)	9.108(3)
c (Å)	11.280(2)	10.923(3)	24.313(4)	24.445(6)
β (deg)	95.02(3)	94.248(18)		
V ($Å^3$)	725.2(3)	688.1(3)	1415.5(4)	1370.5(7)
Z	4	4	8	8
Z'	1	1	2	2
ρ_{calcd} (g cm^{-3})	1.247	1.314	1.278	1.320
μ (mm^{-1})	0.089	0.094	0.092	0.095
$F(000)$	288	288	576	576
θ limits (deg)	3.04 – 29.23	3.64 – 27.56.	1.68 – 27.55	3.33 – 30.70
limiting indices	$-9 \le h \le 10$ $-11 \le k \le 10$ $-15 \le l \le 14$	$-9 \le h \le 9$ $-10 \le k \le 10$ $-12 \le l \le 14$	$-7 \le h \le 7$ $-12 \le k \le 9$ $-28 \le l \le 31$	$-8 \le h \le 8$ $-9 \le k \le 12$ $-34 \le l \le 27$
no. of reflns collected/ unique	5582/1851 [R(int) = 0.0329]	8017/1530 [R(int) = 0.0718]	8805/1897 [R(int) = 0.0369]	10647/4110 [R(int) = 0.0840]
completeness to θ (%)	96.8 (θ = 25.00)	96.5 (θ = 27.56)	99.6 (θ = 27.55)	98.0 (θ = 30.70)
refinement method	full-matrix least-squares on F^2	full-matrix least-squares on F^2	full-matrix least-squares on F^2	full-matrix least-squares on F^2
data/restraints/params	1851/0/111	1530/0/124	3232/0/223	4110/0/245
GOF on F^2	0.989	0.964	0.923	0.952
final R indices [$I > 2\sigma(I)$]	R_1 = 0.0441	R_1 = 0.0420	R_1 = 0.0406	R_1 = 0.0562
R indices (all data)	R_1 = 0.0995	R_1 = 0.1122	R_1 = 0.0987	R_1 = 0.1297
absolute structure param			−0.3(14)	0.1(15)
extinction coeff		0.008(3)		
largest diff. peak and hole (e $Å^{-3}$)	0.111 and −0.125	0.180 and −0.155	0.085 and −0.115	0.192 and −0.170

to 0.1 μg in a Sartorius 4504 Mp8–1 ultramicro balance. The crucible with the sample was transferred to the sample holder in the bomb head. A volume of 50 μL of distilled and deionized water from a Millipore system (conductivity 0.1 μS) was introduced into the bomb body. The stainless-steel bomb of 17.95 cm^3 internal volume was closed and purged twice by successively charging it with oxygen at a pressure of 1.01 MPa and venting the overpressure. After purging, the bomb was filled with oxygen at a pressure of 3.04 MPa and transferred into the calorimeter. The ignition of the sample was initiated by discharge of a 2200 μF capacitor through a platinum wire. The duration of the initial, main, and final periods of the experiment was 30 min each. The HNO_3(aq) formed from traces of atmospheric N_2 remaining inside the bomb after purging with O_2 was determined as NO_3^-, using a Dionex 4000i ion chromatography apparatus. A monoclinic HAP sample of 500 mg pressed into a pellet, left inside a macrocombustion calorimeter[27] for 2 h under conditions similar to those of the microcombustion experiments (3.04 MPa of O_2 and 1 cm^3 of distilled and deionized water inside the bomb), and analyzed by X-ray powder diffraction after grinding, showed no evidence of undergoing a phase transition.

Enthalpy of Sublimation and Vaporization Measurements. The enthalpies of sublimation of forms I and II of HAP were determined using the electrically calibrated twin-cell Calvet microcalorimeter and the operating procedure previously reported.[28,29] In a typical experiment the sample with a mass in the range 2.3−5.2 mg (form I) or 1.7−4.9 mg (form II) was placed into a small glass capillary and weighed with a precision of 1 μg in a Mettler M5 microbalance. The capillary was equilibrated for ca. 10 min, at 298.15 K, inside a furnace placed above the entrance of the sample cell, and subsequently dropped into the cell under a N_2 atmosphere. The temperature of the calorimeter was set to 348.2 K in both cases. In the experiments with form I, an endothermic peak due to the heating of the compound and capillary from 298.15 K to the temperature of the calorimeter was first recorded. Evacuation of the sample and reference cells to 0.13 Pa was started when the signal returned to the baseline and the measuring curve corresponding to the enthalpy of sublimation of the compound at 348.2 K was obtained. In the case of form II, the sample and reference cells were simultaneously evacuated to 0.13 Pa immediately after dropping the sample and the measuring curve due to the heating of the capillary and to the process HAP(cr II, 298.15 K) → HAP(g, 348.2 K) was acquired. The enthalpy of the latter was derived from the area of the curve corresponding to the overall calorimetric event and the calibration constant of the apparatus, after subtracting the contribution associated with the heating of the capillary.[29] The enthalpy of sublimation of form II at 298.15 K could then be calculated by using the heat capacity of the gaseous HAP obtained from density functional theory calculations (see below). No residues were found inside the calorimetric cell at the end of the experiments with forms I and II.

The enthalpy of sublimation of form I was also determined by using the Knudsen effusion apparatus and operating procedure previously described.[30–32] The temperature of the tubular furnace surrounding the brass block containing the effusion cell was controlled to better than ± 0.1 K by a Eurotherm 902P thermostatic unit and a K type thermocouple placed in contact with the inner wall of the furnace. The equilibrium temperature inside the cell was assumed to be identical to the temperature of the brass block. This temperature was measured with a precision of ± 0.1 K by a Tecnisis 100 Ω platinum resistance thermometer embedded in the block and connected in a four wire configuration to a Keithley 2000 multimeter. The cell was initially charged with ca. 0.2 g of sample, and the mass loss in each run was determined to $\pm 1 \times 10^{-5}$ g with a Mettler AT201 balance. A preliminary test where a sample of HAP(cr I) was analyzed by X-ray powder diffraction after being subjected to vacuum conditions similar to those existing in the Knudsen effusion experiments showed no evidence of a phase change.

The experimental procedure used to determine the enthalpy of vaporization of HAP by Calvet microcalorimetry, was similar to that described for the sublimation of form I. The temperature of the calorimeter was set at 385.4 K (above the temperature of fusion of HAP) and the evacuation of the cells was started after the measuring curve corresponding to the heating and fusion of the compound was recorded.

Solution Calorimetry. The enthalpies of solution of forms I and II of HAP in ethanol, at 298.15 K, were measured using an isoperibol Thermometric Precision Solution Calorimeter adapted to a Thermal Activity Monitor thermostat. The apparatus had been previously tested by measuring the enthalpy of solution of tris(hydroxymethyl)aminomethane in 0.05 mol dm^{-3} NaOH and 0.1 mol dm^{-3} HCl.[33,34] The calorimetric cell consisted of a 100 cm^3 Pyrex glass vessel supporting a 30 kΩ thermistor for temperature measurement and a 50 Ω resistance for electrical calibration. The stirrer, which also served as the ampule holder, was operated at 400 rpm. In a typical experiment a thin walled 1 cm^3 glass ampule was loaded with ca. 139 mg of sample and weighed to $\pm 1 \times 10^{-5}$ g in a Mettler AT201 balance. The solution process was started by breaking the ampule in 100 cm^3 of ethanol. Electrical calibrations in which a potential difference of ca. 5 V was applied to the calibration resistance during ca. 27 s, were made before and after the solution process. The energy equivalent of the calorimetric system

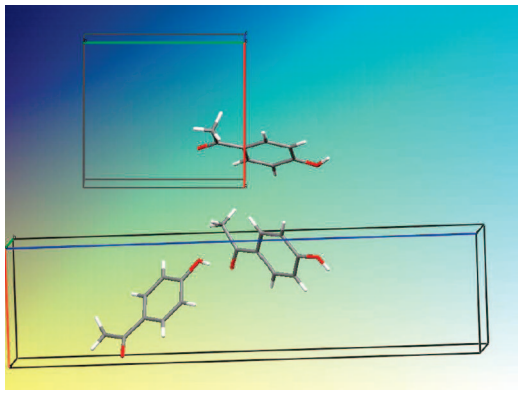

Figure 2. Asymmetric units of 4′-hydroxyacetophenone polymorphs: form I, monoclinic (top); form II, orthorhombic (bottom).

and the adiabatic temperature change[25] were calculated using the SolCal 1.2 program from Thermometric. The heat associated with ampule breaking was not taken into account, since it was found to be negligible in previous experiments where the solvent had a higher vapor pressure than ethanol.[36]

Density Functional Theory (DFT) Calculations. DFT calculations on gaseous HAP were performed using the Gaussian-03 package.[37] Full geometry optimizations and vibration frequency predictions were made using the Becke's three-parameter hybrid method[38] with the Lee, Yang, and Parr LYP[39] correlation functional (B3LYP), and the 6–31G(d,p) basis set.[40] The corresponding molecular energies (E) were obtained from eq 1[41]

$$E = V_{NN} + H^{CORE} + V_{ee} + E_X[\rho] + E_C[\rho] \quad (1)$$

where V_{NN} is the nuclear–nuclear interaction, H^{CORE} is a monoelectronic contribution to the total energy, including electron kinetic and electron–nuclear interaction energies, and V_{ee} is the Coulombic interaction between the electrons. The terms $E_X[\rho]$ and $E_C[\rho]$ represent the exchange and correlation energies, respectively, functionals of the electronic density ρ. The E values were converted to standard enthalpies at 298.15 K by using zero point energy and thermal energy corrections calculated at the same level of theory.

Results and Discussion

Structure. Single-crystal X-ray diffraction analysis of crystals with a tubular morphology, carried out at 298 and 150 K confirmed that a new polymorphic form of HAP was obtained in this work. This new form (form I) is monoclinic, space group $P2_1/c$, and has $Z' = 1$, whereas form II, previously reported[13,14] but also redetermined by us at 298 and 150 K, is orthorhombic, space group $P2_12_12_1$, and has $Z' = 2$. The structural results published for form II at 298 and 150 K are in good agreement with those obtained in this work at the same temperatures. The asymmetric units of the two 4′-hydroxyacetophenone polymorphs are shown in Figure 2 and the Raster3D[22] drawing, with the labeling scheme of the HAP molecules in both phases, is illustrated in Figure 3 for form II.

The bond angles and distances of the HAP molecules in the two polymorphs are similar (Table 2), but the results suggest that the conformation of the hydroxyl group in the molecule of the monoclinic form is not superimposable with those found in the two molecules of the orthorhombic form (Figure 4).

The packing diagrams of the two phases at 298 K are rather different, although the O−H···O hydrogen bonds present in both cases are of the same type: they involve "head-to-tail" bonding between the hydroxyl group of one molecule (donor) and the carbonyl group of an adjacent molecule (acceptor).

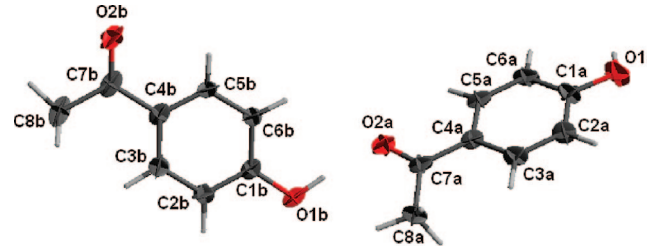

Figure 3. Raster3D[22] drawing and labeling scheme of the 4′-hydroxyacetophenone molecule. The diagram refers to the molecular conformation of form II, but the labeling scheme is analogous for form I.

As shown in Figure 5a (see also Table 3 for intermolecular distances) the crystalline structure of form I at 298 K exhibits infinite linear chains C(8) along the b axis, sustained by O1−H···O2 hydrogen bonds ($d_{OH\cdots O} = 1.82$ Å; $d_{O\cdots O} = 2.68$ Å). These chains are arranged parallel to the (−101) plane and do not interact among themselves (Figure 5b). They are also almost superimposed in a direction perpendicular to this plane, the interchain separation being 3.50 Å. The superposition is in such a way that the carboxyl group in one chain is positioned over the C−C bond of the aromatic ring that is nearest to the hydroxyl group in the adjacent layer (Figures 5c). This packing precludes the formation of an efficient $\pi-\pi$ stacking but, on the other hand, the opposite orientation of the molecules in the chains of two different layers favors the cancelation of the large dipole moment exhibited by HAP in the conformation of form I. According to the results of B3LYP/6–31G(d,p) calculations the dipole moment of HAP is $\mu = 4.35$ D in the conformation of form I and $\mu = 2.61$ D in the conformation form II.

In the crystal structure of form II at 298 K, the planes containing the two symmetry independent molecules of the unit cell make a dihedral angle of 58.5°. These molecules form a O−H···O hydrogen bond ($d_{OH\cdots O}$= 1.64 Å; $d_{O\cdots O} = 2.71$ Å) involving the hydrogen atom of an hydroxyl group and the oxygen atom of the carbonyl group of an adjacent molecule (Figure 6a). This bimolecular motif binds to a similar one through a longer hydrogen bond of the same type ($d_{OH\cdots O} =$ 1.80 Å; $d_{O\cdots O} = 2.74$ Å), building a C(8) helicoidal chain along the c axis (Figure 6b). The helicoidal chain links to analogous chains through C5aH···O1b ($d_{CH\cdots O}$= 2.49 Å), C8bH···O1a ($d_{CH\cdots O}$= 2.68 Å), and C8bH···O2b ($d_{CH\cdots O}$= 2.66 Å) interactions (Figure 6c) forming a 3D supramolecular structure.

A contraction of the unit-cell volume (Table 1), without significant changes in the supramolecular structure, is observed for both forms when the temperature decreases to 150 K. In the case of form I, the C(8) chains along the b axis present at 298 K are also found at 150 K, although with somewhat shorter O−H···O hydrogen bonds ($d_{OH\cdots O} = 1.73$ Å cf $d_{OH\cdots O} = 1.82$ Å; $d_{O\cdots O} = 2.66$ Å cf $d_{O\cdots O} = 2.68$ Å; Table 3). In the lower temperature structure, the oxygen of the hydroxyl group also establishes a weaker intermolecular interaction of C3−H···O1 type ($d_{CH\cdots O} = 2.72$ Å), considering the difference, Δ, between the H···O distance and the sum of the van der Waals radii[23] of H and O (Δ = −0.004 Å, Table 3) an indication of the strength of contact interactions. This interaction, which is not present at 298 K, generates infinite 2D ribbons parallel to the (−101) planes (Figure 7). Although the interplanar separation between these 2D ribbons along the a axis is relatively small (3.398 Å for C2···C7), the strength of the contact is also weak (Δ = −0.002 Å, Table 3). In the case of form II, no new interactions appear on cooling to 150 K, the most notable feature being the

Table 2. Geometrical Parameters of the Structures of Forms I and II Obtained at Different Temperatures

	form I (T = 298 K)	form I (T = 150 K)	form II (T = 298 K)	form II (T = 150 K)
		Bond Distance (Å)		
O1−C1	1.370(2)	1.352(2)	1.359(3), 1.351(3)	1.353(3), 1.356(3)
C2−C1	1.382(2)	1.385(3)	1.379(4), 1.380(4)	1.393(3), 1.383(3)
C2−C3	1.383(2)	1.386(3)	1.371(4), 1.372(4)	1.372(4), 1.375(3)
C3−C4	1.395(2)	1.391(3)	1.378(3), 1.368(4)	1.392(3), 1.382(3)
C5−C4	1.402(2)	1.395(3)	1.387(3), 1.375(4)	1.392(3), 1.382(3)
C5−C6	1.378(2)	1.378(3)	1.370(4), 1.366(4)	1.373(3), 1.375(3)
C1−C6	1.389(2)	1.396(3)	1.372(4), 1.362(4)	1.385(3), 1.375(3)
C7−C4	1.486(2)	1.473(3)	1.465(3), 1.471(4)	1.471(3), 1.473(3)
C7−C8	1.492(3)	1.492(3)	1.494(4), 1.493(4)	1.493(4), 1.497(4)
C7−O2	1.231(2)	1.230(2)	1.226(3), 1.224(3)	1.229(3), 1.223(3)
		Bond Angle (deg)		
O1−C1−C2	122.9(1)	122.8(2)	117.5(3), 118.2(2)	117.4(2), 118.3(2)
O1−C1−C6	117.1(2)	116.9(2)	122.7(2), 122.6(2)	123.3(2), 121.9(2)
C3−C2−C1	119.7(1)	119.5(2)	119.8(3), 120.0(3)	120.1(2), 119.8(2)
C2−C3−C4	121.6(2)	121.2(2)	121.2(3), 121.3(3)	121.1(2), 121.3(2)
C5−C4−C3	117.6(1)	118.3(2)	118.1(2), 117.6(2)	118.0(2), 117.9(2)
C6−C5−C4	121.1(1)	121.3(2)	121.0(2), 121.8(3)	121.3(2), 121.5(2)
C6−C1−C2	120.0(1)	120.2(2)	119.7(2), 119.1(3)	119.3(2), 119.7(2)
C1−C6−C5	120.0(2)	119.5(2)	120.1(2), 120.1(3)	120.1(2), 119.8(2)
C5−C4−C7	119.3(1)	119.2(2)	119.4(2), 120.3(3)	119.3(2), 120.1(2)
C3−C4−C7	123.1(2)	122.5(2)	122.4(2), 122.0(2)	122.7(2), 122.0(2)
C4−C7−C8	120.0(2)	120.1(2)	120.1(3), 119.4(3)	119.3(2), 118.6(2)
O2−C7−C4	120.0(2)	120.2(2)	120.5(2), 120.5(3)	120.9(2), 120.9(2)
O(2)−C(7)−C(8)	120.0(2)	119.7(2)	119.4(2), 120.1(3)	119.8(2), 120.5(2)

contraction of the O···O and C···O distances associated with the O−H···O and C−H···O hydrogen bonds (Table 3).

Form II with a 3D arrangement has a higher density than form I (Table 1: 1.320 g cm^{-3} cf. 1.314 g cm^{-3} at 150 K and 1.278 g cm^{-3} cf. 1.247 g cm^{-3} at 298 K), even though the packing fractions[42,43] of both polymorphs are very similar (ca. 0.70) independently of the temperature considered. This indicates that the HAP system obeys, to Kitaigorodskii's "density rule", according to which the most stable polymorph should correspond to the structure with the highest density.[2,44] As unequivocally shown by the results of the calorimetric measurements described below, at 298 K, the higher density form II has a higher lattice enthalpy and is more stable from the thermodynamic point of view than form I.

It is also noted that the fact that form II has a greater Z' than the less stable form I contrasts with the recent suggestion that high Z' structures are metastable precursors of more stable lower Z' forms along the crystallization pathway.[45,46] The generality of this hypothesis has been questioned[47,48] and possible exceptions have been admitted if directional interactions such as hydrogen bonds are present.[46] The structural data in Table 3 do not show a clear trend to support an increased stabilization of form II relative to form I due to O−H···O hydrogen bonding: at 150 and 298 K, the thermodynamically more stable form II (Z' = 2) exhibits longer O···O distances (decreasing bond strength) and O−H···O angles closer to 180° (increasing bond strength) than the analogous distances and angles in form I (Z' = 1). The C−H···O interactions are, however, stronger (shorter CH···O distances) and more numerous in form II. On the basis of a statistical analysis of data in the Cambridge Structural Database,[49] Babu and Nangia[50] remarked that high Z′ structures tend to have shorter C−H···O interactions than their low Z' counterparts, and they hypothesized that these interactions, although weak, may be responsible for the existence of high Z' structures that are more stable than their corresponding low Z' polymorphs. In line with this view we may speculate that, in the case of HAP, the larger stability of form II relative to form I, at 298 K, is perhaps related to the differences in C−H···O interactions.

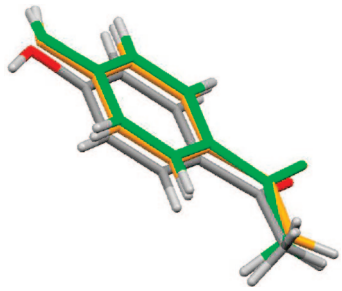

Figure 4. Conformation of the molecules in forms I (grey) and II (yellow and green) of 4′-hydroxyacetophenone, suggested by the X-ray diffraction analysis.

Energetics. The 2005 IUPAC recommended standard atomic masses were used in the calculation of all molar quantities.[51] It was also assumed throughout the discussion, that the influence of pressure on the enthalpies of phase transitions was negligible, and that the obtained experimental results could, therefore, be identified with standard molar values (p = 1 bar).[52]

No phase transitions were observed in the DSC curve of monoclinic HAP (form I) between 283 K and the fusion temperature. The onset and the maximum temperatures of the fusion peak were T_{on} = 381.9 ± 0.1 K and T_{max} = 382.8 ± 0.1 K (Figure 8). The corresponding enthalpy of fusion was $\Delta_{fus}H^{o}_{m}$(HAP, cr I) = 18.08 ± 0.07 kJ mol^{-1}. The uncertainties quoted for T_{on}, T_{max} and $\Delta_{fus}H^{o}_{m}$ correspond to twice the standard error of five independent determinations. In the case of the orthorhombic polymorph (form II) a broad endothermic peak with onset at 351.2 ± 2.7 K (mean of eight determinations) was detected before fusion (Figure 8). X-ray diffraction analysis carried out on two form II samples kept in an oven for 24 h at 343 and 373 K, respectively (below and above the phase transition temperature; Figure 9), enabled the assignment of that peak to the form II → form I transition, for which the DSC experiments gave $\Delta_{trs}H^{o}_{m}$(II → I) = 0.53 ± 0.06 kJ mol^{-1}. Hence, these results indicate that although the two polymorphs

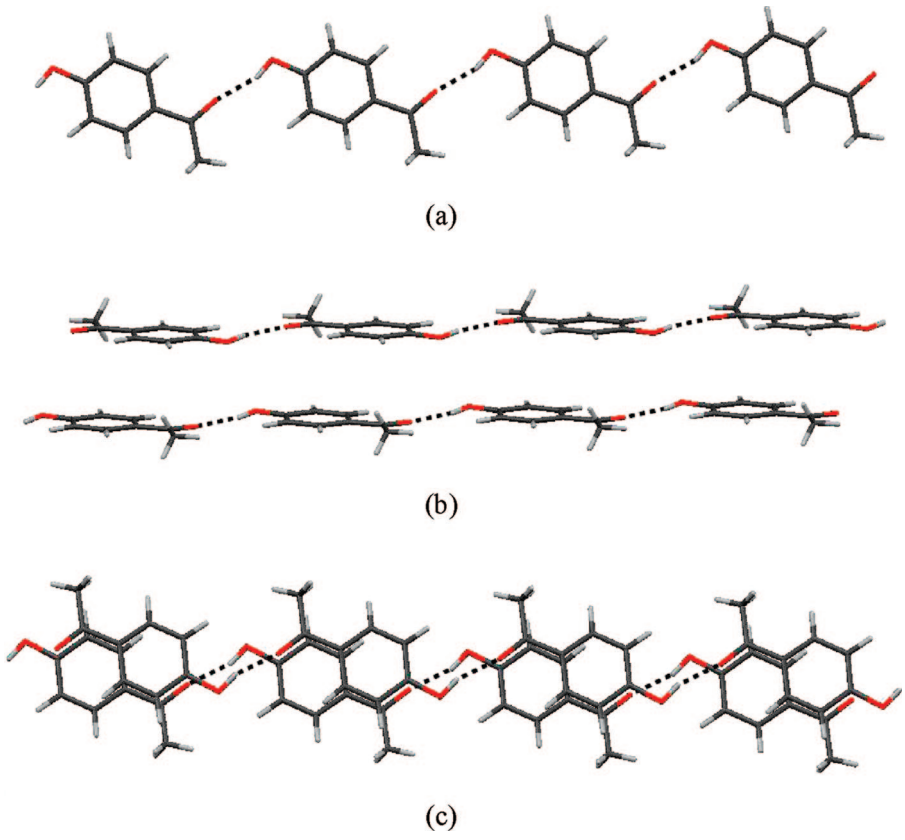

Figure 5. Crystal packing of monoclinic 4′-hydroxyacetophenone (form I) at 298 K. (a) C(8) chain viewed along the *b* axis. (b) Infinite chains parallel to the (−101) plane. (c) View perpendicular to the (−101) plane.

Table 3. O−H···O and C−H···O Interactions and C−H···O Angle for the Two Polymorphs of 4′-Hydroxyacetophenone at 298 and 150 K[a]

	O···O or C···O distance (Å)		H···O distance (Å)		O−H···O or C−H···O angle (deg)		Δ (Å)[a]	
interaction	298 K	150 K	298 K	150 K	298 K	150 K	298 K	150 K
				Form I				
O1−H1···O2	2.676(2)	2.659(2)	1.82(2)	1.73(3)	160(2)	162(3)	−0.900	−0.989
C3−H3···O1		3.375(3)		2.72(2)		125(1)		−0.004
C2···C7		3.398(3)						−0.002
				Form II				
O1b−H01b···O2a	2.707(2)	2.703(3)	1.64(3)	1.82(3)	178(3)	174(4)	−1.079	−0.908
O1a−H01a···O2b	2.739(3)	2.730(3)	1.80(3)	1.92(3)	166(3)	168(4)	−0.925	−0.802
C5a−H5a···O1b	3.383(3)	3.277(3)	2.49(2)	2.50(3)	146(2)	140(3)	−0.212	−0.219
C8b−H8d···O1a	3.488(5)	3.458(5)	2.68(1)	2.52(5)	142(1)	144(4)	−0.042	−0.203
C8b−H8f···O2b	3.582(4)	3.546(4)	2.66(1)	2.73(3)	161(1)	150(3)	−0.056	0.007

[a] Difference between the H···O distance in column 4 and the sum of the van der Waals radii of H and O.[23]

can coexist at ambient temperature, they are enantiotropically related: on heating from ambient temperature, form II is first converted into form I at 351.2 ± 2.7 K, followed by fusion of form I at 381.9 ± 0.1 K.

The relative thermodynamic stability of both phases above 298.15 K was characterized by various calorimetric methods. Microcombustion calorimetry was used to determine the standard molar enthalpy of formation of monoclinic HAP at 298.15 K. This method first led to the corresponding standard molar enthalpy of combustion at 298.15 K as $\Delta_c H^o_m$(HAP, cr I) = −3922.511 ± 1.60 kJ mol^{-1} (see the Supporting Information for details), where the uncertainty quoted represents twice the overall standard error of five independent results and includes the contributions from the energy of combustion of benzoic acid and from the calibration experiments.[53] The above value refers to the reaction in eq 2

$$C_8H_8O_2(\text{cr I}) + 9O_2(g) = 8CO_2(g) + 4H_2O(l) \qquad (2)$$

and leads to $\Delta_f H^o_m$(HAP, cr I) = −368.9 ± 1.9 kJ mol^{-1} by using $\Delta_f H^o_m(CO_2, g)$ = −393.51 ± 0.13 kJ mol^{-1} [54] and $\Delta_f H^o_m(H_2O, l)$ = −285.830 ± 0.040 kJ mol^{-1}.[54] Previously to our work, only one determination of the enthalpy of combustion of HAP, $\Delta_c H^o_m$(HAP, cr) = −3930.9 ± 3.9 kJ mol^{-1},[55] had been reported. This value differs from the result indicated above by 8.4 kJ mol^{-1}. It refers, however, to 293 K, it does not include the contribution from the standard state corrections,[56] and no details of the chemical purity and phase purity of the sample were given by the authors.

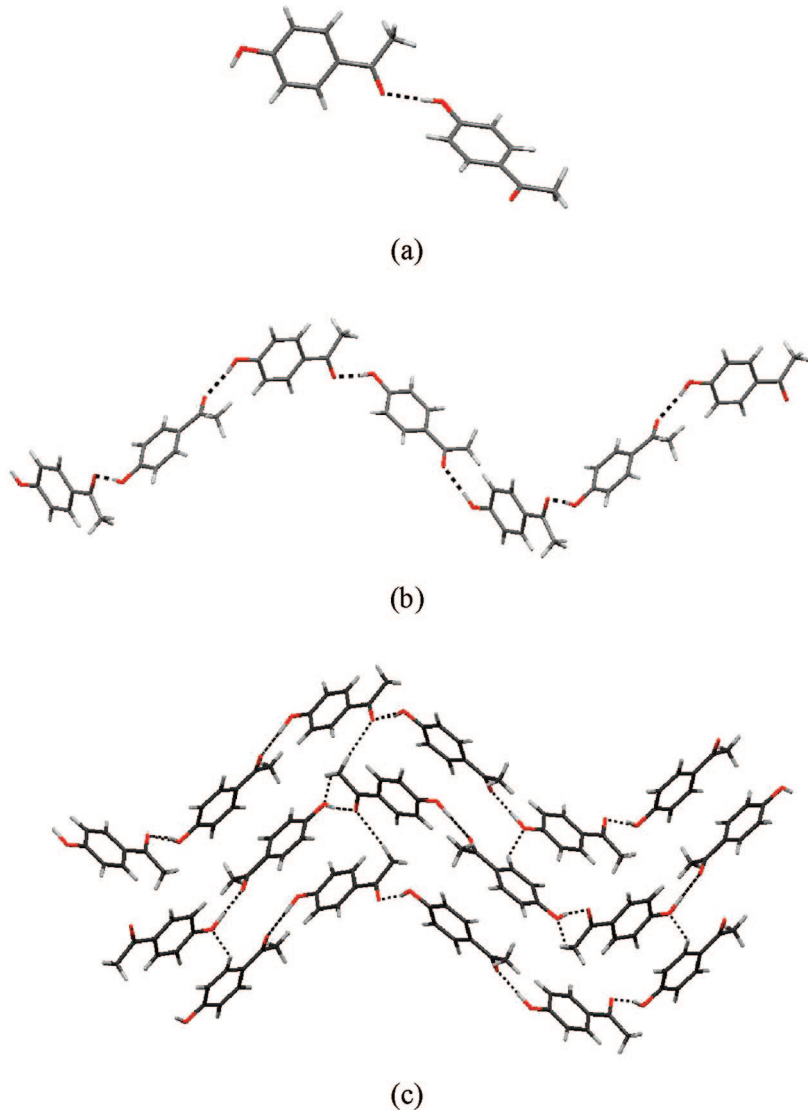

Figure 6. Crystal packing of orthorhombic 4′-hydroxyacetophenone (form II) at 298 K: (a) the two independent molecules in the asymmetric unit linked by a hydrogen bond; (b) helicoidal chains formed through hydrogen bonds along the *c* axis; (c) 3D supramolecular structure generated by the CH···O interactions between the helicoidal chains.

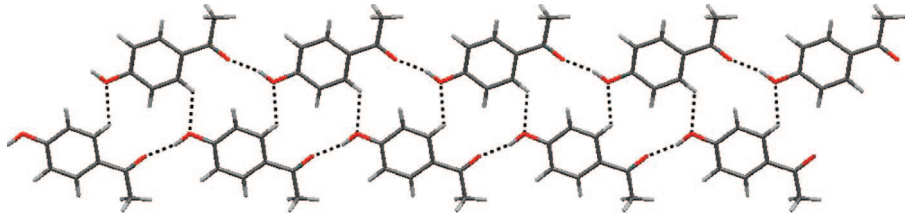

Figure 7. View along the *a* axis of the 2D ribbons generated by C3−H···O1 intermolecular interactions in the monoclinic structure of 4′-hydroxyacetophenone (form I) at 150 K.

To obtain the difference between the enthalpies of formation of the two HAP polymorphs at 298.15 K, and therefore, the enthalpy of the HAP(cr II) → HAP(cr I) close to ambient temperature, the enthalpies of solution of forms I and II in ethanol, to give solutions with approximately identical concentrations (0.0102 mol dm^{-3}; see the Supporting Information for details), were measured by solution calorimetry. These experiments led to $\Delta_{sln}H^{o}_{m}$(HAP, cr I) = 13.72 ± 0.06 kJ mol^{-1} and $\Delta_{sln}H^{o}_{m}$(HAP, cr II) = 14.21 ± 0.12 kJ mol^{-1}, where the indicated uncertainties represent twice the overall standard error of five independent results. Hence $\Delta_{trs}H^{o}_{m}$(II → I) = 0.49 ± 0.13 kJ mol^{-1}, confirming that the endothermic nature of the transition HAP(cr II) → HAP(cr I) observed by DSC at 351.2 ± 2.7 K also extends to 298.15 K. It is therefore concluded that on enthalpic grounds, the orthorhombic phase is also more stable than the monoclinic phase at ambient temperature.

Combining the results of the combustion and solution calorimetry studies, it was possible to derive the enthalpy of formation of orthorhombic HAP at 298.15 K as $\Delta_{f}H^{o}_{m}$(HAP, cr II) = $\Delta_{f}H^{o}_{m}$(HAP, cr I) + $\Delta_{sln}H^{o}_{m}$(HAP, cr I) − $\Delta_{sln}H^{o}_{m}$(HAP, cr II) = −369.4 ± 1.9 kJ mol^{-1}.

Further evidence for the consistency of the above conclusions regarding the endothermicity of the II → I transition, and the enantiotropic nature of the HAP system, was provided by measurements of enthalpies of sublimation using Knudsen effusion and Calvet microcalorimetry. The vapor pressure, p, of monoclinic HAP (form I) obtained in the range 318.2−338.4 K by Knudsen effusion (see the Supporting Information) was calculated from[57,58]

$$p = \frac{m}{At}\left(\frac{2\pi RT}{M}\right)^{1/2}\left(\frac{8r+3l}{8r}\right)\left(\frac{2\lambda}{2\lambda+0.48r}\right) \quad (3)$$

where m is the mass loss during the time t; A, l, and r are the area, the thickness, and the radius of the effusion hole, respectively; M is the molar mass of the compound under study, R is the gas constant, T is the absolute temperature, and λ is the mean free path given by[59]

$$\lambda = \frac{kT}{\sqrt{2}\pi\sigma^2 p} \quad (4)$$

Here k represents the Boltzmann constant and σ the collision diameter. The collision diameter of gaseous HAP was estimated as 6.18 Å, from the van der Waals volume of the molecule calculated with the GEPOL93 program.[60] The van der Waals radii of carbon (1.70 Å), hydrogen (1.20 Å), and oxygen (1.52 Å) given by Bondi were selected for this calculation.[61] The dimensions of the effusion hole were $A = 2.27 \times 10^{-7}$ m^2, $l = 2.09 \times 10^{-5}$ m, and $r = 2.688 \times 10^{-4}$ m. The vapor pressure against temperature data were fitted to eq 5[62]

$$\ln p = a + \frac{b}{T} \quad (5)$$

where the slope b is related to the enthalpy of sublimation at the average of the highest and lowest temperatures of the range covered in each series of experiments, T_m = 327.4 K, by $\Delta_{sub}H^o_m(T_m) = -bR$. The obtained results were $a = 35.20 \pm 0.43$, $b = -12245.9 \pm 146.2$, and $\Delta_{sub}H^o_m$(HAP, cr I, 327.4 K) = 101.8 ± 2.7 kJ mol^{-1}. The uncertainties quoted for a and b are the corresponding standard errors, and that for $\Delta_{sub}H^o_m(T_m)$ includes Student's factor for 95% confidence level (t = 2.201 for 12 independent measurements). The enthalpy of sublimation of HAP at 298.15 K, $\Delta_{sub}H^o_m$(HAP, cr I) = 103.3 ± 2.7 kJ mol^{-1}, was derived from:

$$\Delta_{sub}H^o_m(298.15\ \text{K}) = \Delta_{sub}H^o_m(T) + \int_T^{298.15\ \text{K}} \left[C^o_{p,m}(\text{g}) - C^o_{p,m}(\text{cr})\right] \mathrm{d}T \quad (6)$$

where $C^o_{p,m}$(cr) and $C^o_{p,m}$(g) are the molar heat capacities of the compound in the crystalline and gaseous states, respectively. The calculation was based on the mean value of the heat capacity of monoclinic HAP in the range 298–347 K, $C^o_{p,m}$(HAP, cr I) = 214.8 J K^{-1} mol^{-1}, determined by Calvet-drop microcalorimetry using a previously reported procedure,[29] and on the temperature dependence of the heat capacity of gaseous HAP in the range 200−400 K ($C^o_{p,m}$ in J K^{-1} mol^{-1}):

$$C^o_{p,m}(\text{HAP, g}) = -1.9376 \times 10^{-4}T^2 + 0.5596T + 6.8932 \quad (7)$$

obtained by Statistical Mechanics,[63] using vibration frequencies calculated by the B3LYP/6–31G(d,p) method and scaled by 0.9608.[64]

The enthalpy of sublimation of monoclinic HAP was also measured at 348.0 K, by using Calvet drop microcalorimetry. These experiments led to $\Delta_{sub}H^o_m$(HAP, cr I, 348.0 K) = 100.87 ± 0.82 kJ mol^{-1}, where the uncertainty quoted represents twice the standard error of seven independent results. Correction of this value to 298.15 K, using eq 6 and the heat capacity data indicated above, leads to $\Delta_{sub}H^o_m$(HAP, cr I) = 103.23 ± 0.82 kJ mol^{-1} in good agreement with the corresponding value obtained by the Knudsen effusion method. The weighted mean of the results from both techniques $\Delta_{sub}H^o_m$(HAP, cr I) = 103.2 ± 0.8 kJ mol^{-1} was selected in this work.[64]

The enthalpy of sublimation of orthorhombic HAP at 298.15 K was derived from the enthalpy of the process

$$\text{HAP(cr II, 298.15 K)} \rightarrow \text{HAP(g, 348.1 K)} \quad (8)$$

determined by Calvet drop microcalorimetry. The obtained value was $\Delta H^o_m(8)$ = 112.61 ± 0.39 kJ mol^{-1}, where the indicated uncertainty represents twice the standard error of six independent results. Correction of the final state to 298.15 K using the heat capacity of gaseous HAP given by eq 7, leads to $\Delta_{sub}H^o_m$(HAP, cr II) = 104.3 ± 0.4 kJ mol^{-1}.

The vapor pressure of solid HAP in the range 320.5−348.9 K, had been previously measured by Aihara, using the viscosity gauge method and a sample of undefined phase purity.[65] From his data, it is possible to derive $\Delta_{sub}H^o_m$(HAP) = 95.7 ± 1.5 kJ mol^{-1} at 334.7 K. Correction of this value to 298.15 K, using the heat capacity data selected in this work leads to $\Delta_{sub}H^o_m$(HAP) = 97.5 ± 1.5 kJ mol^{-1}, which is lower by 5.7 kJ mol^{-1} and 6.8 kJ mol^{-1}, respectively, than the standard molar enthalpies of sublimation of forms I and II here reported.

The difference between the enthalpies of sublimation of the two polymorphs of HAP at 298.15 K corresponds to $\Delta_{trs}H^o_m$(II → I) = 0.9 ± 0.9 kJ mol^{-1}, in agreement with the more precise $\Delta_{trs}H^o_m$(II → I) = 0.49 ± 0.13 kJ mol^{-1} obtained from the solution calorimetric studies. Hence, the results of the three calorimetric methods used (DSC, solution calorimetry, and sublimation calorimetry) indicate that the two polymorphs are enantiotropically related and that form II is more stable than form I from ambient temperature to the phase transition temperature.

The values of $\Delta_f H^o_m$(cr) and $\Delta_{sub}H^o_m$ obtained for forms I and II of HAP lead to $\Delta_f H^o_m$(HAP, g) = −265.7 ± 2.1 kJ mol^{-1} and −265.1 ± 1.9 kJ mol^{-1}, respectively. Because these results are within their combined uncertainty intervals, their weighted mean $\Delta_f H^o_m$(HAP, g) = −265.4 ± 1.4 kJ mol^{-1} is recommended in this work.

Phase Diagrams. Two of the most succinct ways of presenting the stability domains of the different phases of a compound are in terms of pressure vs temperature ($p-T$) or Gibbs energy vs temperature ($\Delta_f G^o_m - T$) diagrams.[1,2,5] The thermodynamic data obtained in this work allow those diagrams to be approximately defined for 4′-hydroxyacetophenone.

An estimate of the $p-T$ phase diagram (Figure 10) was obtained as follows. The solid I−gas equilibrium line was calculated by using eq 5. The solid II−solid I curve was modeled by

$$p = \frac{\Delta_{trs}H^o_m}{\Delta_{trs}V^o_m}\ln\frac{T}{T_{trs}} + p_{trs} \quad (9)$$

where $\Delta_{trs}H^o_m$ = 0.53 kJ mol^{-1} is the enthalpy of the form II → form I transition determined by DSC at T_{trs} = 351.2 K and p_{trs} = 1 bar, and $\Delta_{trs}V^o_m = 3.491 \times 10^{-6}$ m^3 mol^{-1} is the corresponding volume change obtained from eqs 10 and 11. These equations were derived from the molar volumes of forms

I and II at 150 and 298 K, obtained from the single crystal X-ray diffraction results in Table 1

$$V_m^o(\text{form I}) = 3.7838\times10^{-8}T + 9.7924\times10^{-5} \quad (10)$$

$$V_m^o(\text{form II}) + 2.2973\times10^{-8}T + 9.9654\times10^{-5} \quad (11)$$

The solid II−solid I line intersects the solid I−gas line (eq 5) at a triple point of coordinates T_{triple}(II−I−g) = 351.0 K and p_{triple}(II−I−g) = 1.365 Pa. These values, in conjunction with the enthalpy of sublimation of orthorhombic HAP at 298.15 K obtained in this work by Calvet microcalorimetry (104.3 ± 0.4 kJ mol^{-1}, see above), were used to estimate the parameters that define the solid II−gas curve through eq 5. In this case, a = 36.05 and b = −12544.4.

The solid I−liquid line was taken as:

$$p = \frac{\Delta_{fus}H_m^o}{\Delta_{fus}V_m^o}\ln\frac{T}{T_{fus}} + p_{fus} \quad (12)$$

where $\Delta_{fus}H_m^o$ = 18.08 kJ mol^{-1} is the enthalpy of fusion determined by DSC at T_{fus} = 381.9 K and p_{fus} = 1 bar, and $\Delta_{fus}V_m^o$ = 1.040 × 10^{-5} m^3 mol^{-1} is the volume change associated with the fusion process. The value of $\Delta_{fus}V_m^o$ was derived from the density of liquid HAP at 382 K (ρ = 1.109 g cm^{-3})[66] and the molar volume of solid I at that temperature obtained from eq 10. The intersection of the solid I−liquid and solid I−gas lines leads to the coordinates of the solid I−liquid–gas triple point as T_{triple}(I−l−g) = 381.9 K and p_{triple}(I−l−g) = 22.97 Pa. These values, together with $\Delta_{vap}H_m^o$(HAP) = 81.07 ± 0.47 kJ mol^{-1} obtained in this work by Calvet microcalorimetry at 385.4 K (the uncertainty quoted is twice the standard error of six determinations), were also used to estimate the parameters defining the liquid–gas line through eq 5. In this case, a = 28.67 and b = −9750.5. Finally, the intersection of the solid II−solid I and solid I−liquid curves leads to the coordinates of the solid II−solid I−liquid triple point as T_{triple}(II−I−l) = 385.0 K and p_{triple}(II−I−l) = 14.03 MPa.

The Gibbs energy, enthalpy, and entropy functions necessary for the construction of the $\Delta_fG_m^o$ vs T diagram illustrated in Figure 11a and the plots of $\Delta_{trs}H_m^o$(II → I), $T\Delta_{trs}S_m^o$(II → I), and $\Delta_{trs}G_m^o$(II → I) as a function of the temperature represented in Figure 11b were calculated from eqs 13–16 (see the Supporting Information for details)

$$\Delta_fG_m^o = \Delta_fH_m^o - TS_m^o \quad (13)$$

$$\Delta_{trs}H_m^o(\text{II}\rightarrow\text{I}) = \Delta_fH_m^o(\text{cr I}) - \Delta_fH_m^o(\text{cr II}) \quad (14)$$

$$\Delta_{trs}S_m^o(\text{II}\rightarrow\text{I}) = S_m^o(\text{cr I}) - S_m^o(\text{cr II}) \quad (15)$$

$$\Delta_{trs}G_m^o(\text{II}\rightarrow\text{I}) = \Delta_fG_m^o(\text{cr I}) - \Delta_fG_m^o(\text{cr II}) = \Delta_{trs}H_m^o(\text{II}\rightarrow\text{I}) - T\Delta_{trs}S_m^o(\text{II}\rightarrow\text{I}) \quad (16)$$

by using the standard molar enthalpy of formation and entropy functions derived as follows. The variation of the enthalpy of formation of form I with the temperature was obtained from

$$\Delta_fH_m^o(\text{HAP, cr I}, T) = \Delta_fH_m^o(\text{HAP, cr I, 298.15 K}) + \Delta_fC_{p,m}^o(\text{cr I})(T - 298.15) \quad (17)$$

where $\Delta_fH_m^o$(HAP, cr I, 298.15 K) is the enthalpy of formation of monoclinic HAP at 298.15 K determined in this work (−368.9 ± 1.9 kJ mol^{-1}); the term $\Delta_fC_{p,m}^o$(cr I) = −5.36 J K^{-1} mol^{-1} represents the heat capacity change associated with the formation of monoclinic HAP from O_2(g), H_2(g), and graphite(s). It was calculated from

$$\Delta_fC_{p,m}^o(\text{cr I}) = C_{p,m}^o(\text{HAP, cr I}) - C_{p,m}^o(O_2, \text{g}) - 4C_{p,m}^o(H_2, \text{g}) - 8C_{p,m}^o(\text{C, graphite}) \quad (18)$$

on the basis of the mean heat capacity of monoclinic HAP in the range 298.0 - 347.0 K obtained in this work, $C_{p,m}^o$(cr I) = 214.8 J K^{-1} mol^{-1}, and the mean heat capacities of O_2(g), H_2(g), and graphite(s) in the same temperature range calculated from literature data: $C_{p,m}^o(O_2, \text{g})$ = 29.40 J K^{-1} mol^{-1},[67] $C_{p,m}^o(H_2, \text{g})$ = 28.97 J K^{-1} mol^{-1},[67] $C_{p,m}^o$(C, graphite) = 9.36 J K^{-1} mol^{-1}.[68]

The variation of the enthalpy of formation of form II with the temperature was taken as

$$\Delta_fH_m^o(\text{HAP, cr II}, T) = \Delta_fH_m^o(\text{HAP, cr I, 298.15 K}) - \Delta_{trs}H_m^o(298.15\text{ K}) + \Delta_fC_{p,m}^o(\text{cr II})(T - 298.15) \quad (19)$$

where $\Delta_fH_m^o$(HAP, cr I, 298.15 K) is the enthalpy of formation of monoclinic HAP at 298.15 K mentioned above (−368.9 ± 1.9 kJ mol^{-1}), $\Delta_{trs}H_m^o$(298.15 K) represents the enthalpy of the II → I transition at 298.15 K obtained from the solution calorimetry studies (0.49 ± 0.13 kJ mol^{-1}), and $\Delta_fC_{p,m}^o$(cr II) is the heat capacity change associated with the formation of orthorhombic HAP from O_2(g), H_2(g), and graphite(s). The value of $\Delta_fC_{p,m}^o$(cr II) = −6.11 J K^{-1} mol^{-1} was obtained from

$$\Delta_fC_{p,m}^o(\text{cr II}) = \frac{\Delta_{trs}H_m^o(298.15\text{ K}) - \Delta_{trs}H_m^o(351.2\text{ K}) + \Delta_fC_{p,m}^o(\text{cr I})(351.2 - 298.15)}{351.2 - 298.15} \quad (20)$$

The variation of the enthalpy of formation of liquid HAP with temperature was computed from

$$\Delta_fH_m^o(\text{HAP, l}, T) = \Delta_fH_m^o(\text{HAP, cr I, 298.15 K}) + \Delta_fC_{p,m}^o(\text{cr I})(381.9 - 298.15) + \Delta_{fus}H_m^o + \Delta_fC_{p,m}^o(\text{l})(T - 381.9) \quad (21)$$

The values of $\Delta_fH_m^o$(HAP, cr I, 298.15 K), $\Delta_fC_{p,m}^o$(cr I), and $\Delta_{fus}H_m^o$ were already mentioned above and $\Delta_fC_{p,m}^o$(l) = 29.81 J K^{-1} mol^{-1} was derived from an equation analogous to eq 18 by using $C_{p,m}^o$(l) = 267.7 J K^{-1} mol^{-1} [69] and $C_{p,m}^o(O_2, \text{g})$ = 30.33 J K^{-1} mol^{-1},[67] $C_{p,m}^o(H_2, \text{g})$ = 29.15 J K^{-1} mol^{-1},[67] $C_{p,m}^o$(C, graphite) = 11.37 J K^{-1} mol^{-1}, at 381.9 K.[68]

To obtain the absolute entropies of HAP in the two solid phases and in the liquid state as a function of the temperature, the standard molar entropy of form I at the temperature T_m = 327.4 K was first calculated from:

$$S_m^o(\text{HAP, cr I}, T_m) = S_m^o(\text{g}, T_m) - R\ln\frac{p_{sat}}{p^o} - \frac{\Delta_{sub}H_m(T_m)}{T_m} \quad (22)$$

where $\Delta_{sub}H_m(T_m)$ = 101.8 ± 2.7 kJ mol^{-1} is the enthalpy of sublimation of monoclinic HAP at T_m and at the saturation pressure p_{sat} = 0.1104 Pa, determined by Knudsen effusion. The standard molar entropy of gaseous HAP at T_m, S_m^o(g, T_m) = 408.758 J K^{-1} mol^{-1}, was obtained from

$$S_m^o(\text{HAP, g}) = 1.65499\times10^{-4}T^2 + 0.621999T + 222.855 \quad (23)$$

which results from a polynomial fit to the values of the standard molar entropies of gaseous HAP obtained by statistical ther-

modynamics calculations,[63] using structural data and vibration frequencies predicted by the B3LYP/6–31G(d,p) method (see the Supporting Information). The frequencies were scaled by 0.9608.[64] The internal rotation of the methyl group was considered as hindered. Its contribution for the entropy of gaseous HAP was taken from the tables of Pitzer and Gwin[70] and based on a potential barrier height $V = 5.5$ kJ mol^{-1} calculated from a potential energy surface scan at the B3LYP/6–31G(d,p) level (see the Supporting Information). It should be noted that the derivation of eq 22 is based on the hypothesis that the entropy of HAP(cr I) at T_m is the same under standard state conditions (1 bar) and at the saturation pressure $p_{sat} = 0.1104$ Pa; the term $S^o_m(g, T_m) - R\ln(p_{sat}/p^o)$ corresponds to the molar entropy of gaseous HAP at T_m and p_{sat}, assuming ideal gas behavior.

The value of $S^o_m(\text{HAP, cr I}, T_m) = 211.850$ J K^{-1} mol^{-1} obtained from eq 22 was used as an anchor to derive the standard molar entropy of form I as a function of the temperature from

$$S^o_m(\text{HAP, cr I}, T) = S^o_m(\text{HAP, cr I}, T_m) + C^o_{p,m}(\text{cr I}) \ln \frac{T}{T_m} \quad (24)$$

where $C^o_{p,m}(\text{cr I}) = 214.8$ J K^{-1} mol^{-1} represents the standard molar heat capacity of monoclinic HAP mentioned above.

The entropy of form II was obtained from

$$S^o_m(\text{HAP, cr II}, T) = S^o_m(\text{HAP, cr I}, T_{trs}) - \frac{\Delta_{trs}H^o_m(T_{trs})}{T_{trs}} + C^o_{p,m}(\text{cr II}) \ln \frac{T}{T_{trs}} \quad (25)$$

where $S^o_m(\text{HAP, cr I}, T_{trs}) = 226.973$ J K^{-1} mol^{-1} is the entropy of form I at the temperature of the II → I phase transition ($T_{trs} = 351.2$ K), obtained from eq 24. The values $\Delta_{trs}H^o_m(T_{trs}) = 0.53 \pm 0.06$ kJ mol^{-1} and $C^o_{p,m}(\text{cr II}) = C^o_{p,m}(\text{cr I}) + \Delta_f C^o_{p,m}(\text{cr II}) - \Delta_f C^o_{p,m}(\text{cr I}) = 214.1$ J K^{-1} mol^{-1} were also used in the calculations.

Finally, the entropy of liquid HAP was calculated from

$$S^o_m(\text{HAP, l}, T) = S^o_m(\text{HAP, cr I}, T_{fus}) + \frac{\Delta_{fus}H^o_m(T_{fus})}{T_{fus}} + C^o_{p,m}(\text{l}) \ln \frac{T}{T_{fus}} \quad (26)$$

by using $T_{fus} = 381.9$ K, $\Delta_{fus}H^o_m(T_{fus}) = 18.08 \pm 0.07$ kJ mol^{-1}, $C^o_{p,m}(\text{l}) = 267.7$ J K^{-1} mol^{-1},[69] and $S^o_m(\text{HAP, cr I}, T_{fus}) = 244.974$ J K^{-1} mol^{-1} obtained from eq 22.

The general view about the relation between the different phases of 4′-hydroxyacetophenone given by the $p-T$ and $\Delta_f G^o_m - T$ diagrams in Figures 10 and 11, can be summarized as follows. The HAP system is enantiotropic. On heating from 298 K, and at ambient pressure (1 bar), the stability order of the two polymorphs is reversed at 351.2 K, with the ensuing transformation of form II (orthorhombic) into form I (monoclinic). This polymorph subsequently melts at 381.9 K. The $p-T$ stability domain of form I is limited by the equilibrium curves connecting three triple points: solid II−solid I−gas at $T = 351.0$ K and $p = 1.365$ Pa; solid I−liquid–gas at $T = 381.9$ K and $p = 22.97$ Pa; and solid II−solid I−liquid at $T = 385.0$ K and $p = 14.03$ MPa. The direct fusion of form II, without previous transformation into form I, is therefore predicted to occur above 385.0 K and 14.03 MPa (Figure 10). The form II → form I phase transition is accompanied by entropy ($\Delta_{trs}S^o_m = 1.51$ J K^{-1} mol^{-1}) and volume increases ($\Delta_{trs}V^o_m = 3.491 \times 10^{-6}$ m^3 mol^{-1}). This is consistent with the transition from a perhaps more "rigid" to a more "loose" crystal structure (form II exhibits a larger number of interactions in the solid state than form I).

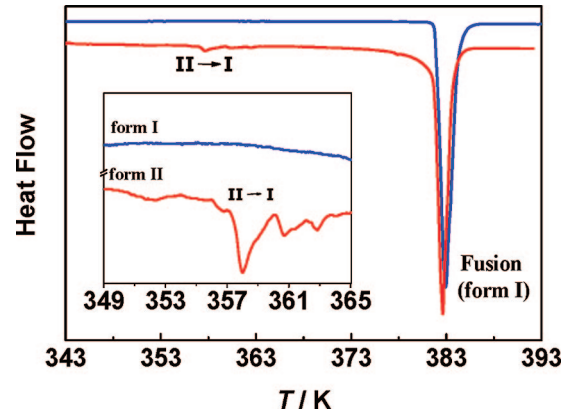

Figure 8. Differential scanning calorimetry measuring curves obtained for the two polymorphs of 4′-hydroxyacetophenone: form I, blue line; and form II, red line. The inset corresponds to expansions of both curves in the II → I phase transition range.

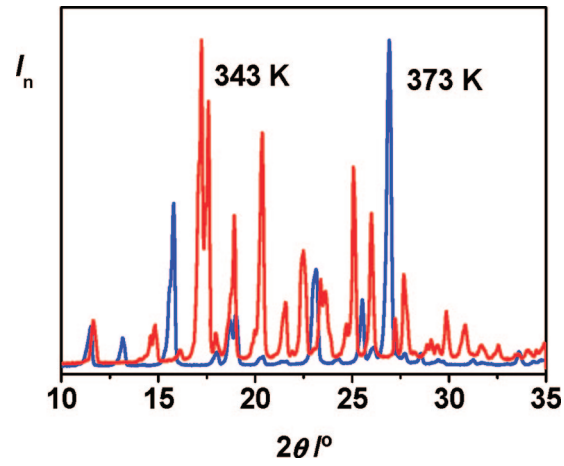

Figure 9. Overlay of the X-ray powder diffractograms of two samples of form II kept in an oven for 24 h at 343 K (curve in red) and 373 K (curve in blue). The powder pattern obtained at 373 K (above the II → I transition temperature) corresponds to that of form I. The intensities were normalized (I_n) relative to the most intense peak observed in each diffractogram.

Our single crystal X-ray diffraction results suggest that the HAP molecules in forms I and II differ by the conformation of the OH group relative to the C(O)CH$_3$ group (Figure 4). It is interesting to note that B3LYP/6–31G(d,p) calculations indicate that $\Delta_{trs}G^o_m(\text{II} \rightarrow \text{I}) \approx \Delta_{trs}H^o_m(\text{II} \rightarrow \text{I}) = 0.7$ kJ mol^{-1} in the gas phase, at 298.15 K. Hence the most stable conformation for the isolated molecule is also that corresponding to the most stable polymorph from a thermodynamic point of view (form II, orthorhombic). Moreover, a potential energy scan performed at the same level of theory led to the conclusion that the barrier for the internal rotation of the OH group associated with the conversion of conformation I into conformation II amounts to 21 kJ mol^{-1} (see the Supporting Information). This large barrier compared to the thermal energy at the temperature of the II → I transition in the solid state ($RT = 2.9$ kJ mol^{-1}, at $T_{trs} = 351.2$ K), suggests that the enantiotropic transformation between the two polymorphs does not involve a simple rotation of the OH group.

Conclusions

A new polymorph of 4′-hydroxyacetophenone (form I, monoclinic, $P2_1/c$, $Z' = 1$), was prepared and characterized.

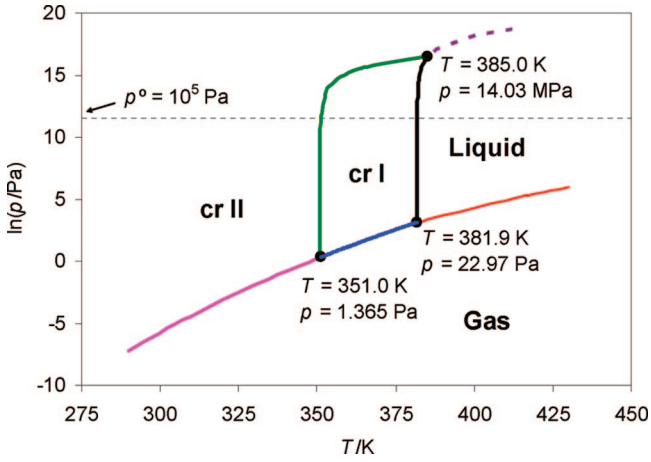

Figure 10. Pressure vs temperature phase diagram for 4′-hydroxyacetophenone. The dotted line is merely indicative of a hypothetical cr II−l equilibrium line.

This new phase exhibits significantly dissimilar packing features from the previously known one (form II, orthorhombic, $P2_12_12_1$, $Z' = 2$). At the molecular level, both phases seem to differ by the conformation of the OH group toward the $C(O)CH_3$ group. Thermodynamic characterization indicates that they are enantiotropically related at ambient pressure, with form II transforming into form I at 351.2 K, followed by fusion of form I at 381.9 K. Direct fusion of form II seems, however, possible at a pressure well above ambient. It is also found that, at 298.15 K, form II is enthalpicaly more stable than form I by ca. 0.5 kJ mol^{-1} and that at the same temperature the estimated Gibbs energy change for the I → II conversion is ca. −0.074 kJ mol^{-1} (Figure 11b). Hence, once monoclinic HAP is formed there is only a slight thermodynamic tendency for its conversion into the orthorhombic phase (the transformation is barely exergonic). Calculations by the B3LYP/6–31G(d,p) method suggest that the conformation corresponding to the more stable form of HAP is also the more stable one when the isolated molecule is considered. In addition, this method predicts that the barrier for the conversion of conformation II into conformation I through a rotation of the OH group is ca. seven times larger than the available thermal energy (RT) at the temperature of the II → I phase transition in the solid state. It is therefore unlikely that this transition involves a simple rotation of the OH group. The combination of a small thermodynamic tendency with a sufficiently large kinetic barrier associated with the phase transition pathway, must therefore be responsible for the fact that monoclinic HAP can be stored at ambient temperature and pressure for long periods of time without transforming into the orthorhombic form. Finally, the fact that the thermodynamically more stable form II of HAP has a greater Z' than the less stable form I, contrasts with the recent proposal that, high Z' structures are metastable precursors of their presumed more stable low Z' forms along the crystallization pathway.

Acknowledgment. This work was supported by Fundação para a Ciência e a Tecnologia, Portugal. A grant from Fundação para a Ciência e a Tecnologia (SFRH/BD/12329/2003) is also gratefully acknowledged by C.E.S.B. We thank Professors Filomena Martins (FCUL, Portugal) and Hermínio Diogo (IST, Portugal) for the use of the solution and microcombustion calorimeters in their laboratories and Prof. J. M. Nogueira (FCUL, Portugal) for the GC-MS analysis. Thanks are also due to Janine Schwiertz and Henning Urch for the recording of the SEM images at Professor Matthias Epple laboratory (University of Duisburg-Essen, Germany).

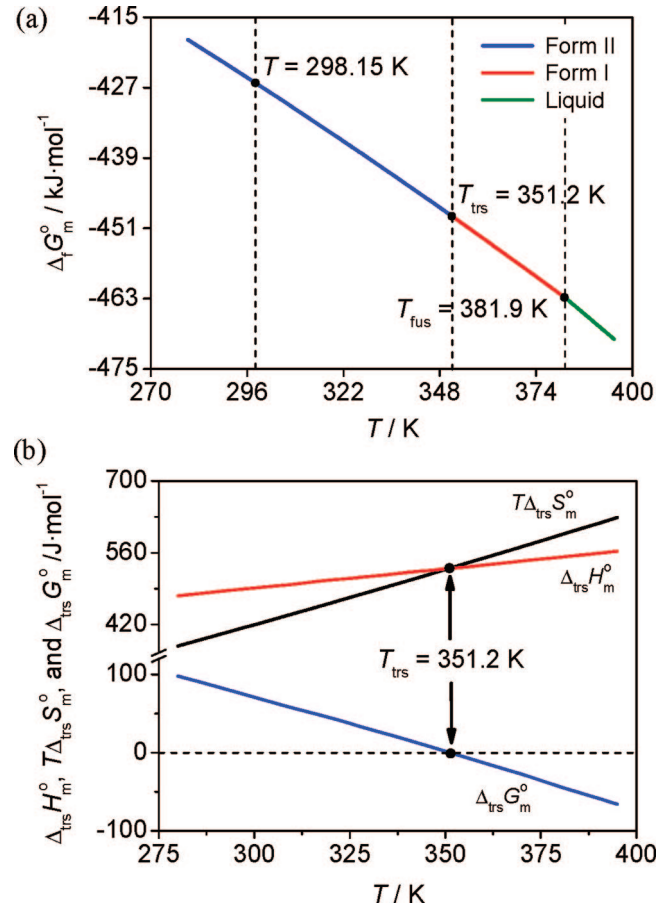

Figure 11. (a) $\Delta_f G^o_m - T$ diagram for the solid and liquid phases of 4′-hydroxyacetophenone. (b) Standard molar Gibbs energy, enthalpy, and entropy of the II → I phase transition as a function of the temperature.

Supporting Information Available: CIF files with the crystallographic parameters and structural data for the monoclinic (form I) and orthorhombic (form II) phases of 4′-hydroxyacetophenone at 150 and 298 K. Tables S1−S3 with the indexation of the powder diffraction lines for the solid compounds studied in this work. Details of the combustion calorimetry (Table S4) and solution calorimetry (Tables S5 and S6) experiments. Table S7 containing the experimental vapor pressures of form I obtained by the Knudsen effusion measurements. Table S8 with the results of the B3LYP/6–31G(d,p) calculations on HAP. Table S9−S11 with the details of the Statistical Mechanics calculations on gaseous HAP. Figure S1 with the labeling scheme used in the calculation of the energy barriers for internal rotation of the CH_3 and OH groups in HAP. Table S12 and Figure S2, with the results of the calculation of the internal rotation barrier of the methyl group in HAP. Table S13 and Figure S3, with the results of the calculation of the internal rotation barrier of the hydroxyl group in HAP. Tables S14 and S15 with the details of the calculations of the $\Delta_f G^o_m - T$ diagram and the plots of $\Delta_{trs}H^o_m$(II → I), $\Delta_{trs}S^o_m$(II → I), and $\Delta_{trs}G^o_m$(II → I) as a function of the temperature in Figure 11 (PDF). This material is available free of charge via the Internet at http://pubs.acs.org.

References

(1) Brittain, H. G. *Polymorphism in Pharmaceutical Solids*; Marcel Dekker: New York, 1999.

(2) Bernstein, J. *Polymorphism in Molecular Crystals*; Oxford University Press: Oxford, U.K., 2002.

(3) Mullin, J. W. *Crystallization*; 4th ed.; Butterworth-Heinemann: Oxford, U.K., 2001.

(4) Gavezzotti, A. *Theoretical Aspects and Computer Modelling of the Molecular Solid State*; John Wiley: Chichester, U.K., 1997.

(5) Westrum, E. F., Jr.; McCullough, J. P. Thermodynamics of Crystals. In *Physics and Chemistry of the Organic Solid State*; Fox, D., Labes, M. M., Weissberger, A. Eds.; Interscience: New York, 1963; *Vol. I.*
(6) Giron, D. *Thermochim. Acta* **1995**, *248*, 1–59.
(7) Giron, D. *J. Thermal Anal. Cal.* **2001**, *64*, 37–60.
(8) Yu, L. *J. Pharm. Sci.* **1995**, *84*, 966–974.
(9) Yu, L.; Huang, J.; Jones, K. J. *J. Phys. Chem. B* **2005**, *109*, 19915–19922.
(10) Toscani, S. *Thermochim. Acta* **1998**, *321*, 73–79.
(11) Grunenberg, A.; Henck, J.-O.; Siesler, H. W. *Int. J. Pharm.* **1996**, *129*, 147–158.
(12) Vainshtein, B. K.; Lobanova, G. M.; Gurskaya, G. V. *Krystallografiya* **1974**, *19*, 531–538.
(13) Chenthamarai, S.; Jayaraman, D.; Meera, K.; Santhanaraghavan, P.; Subramanian, C.; Bocelli, G.; Ramasamy, P. *Cryst. Eng.* **2001**, *4*, 37–48.
(14) Kresge, A. J.; Lough, A. J.; Zhu, Y. *Acta Crystallogr., Sect. E* **2002**, *58*, o1057–o1059.
(15) Laugier, J.; Bochu, B. *Checkcell*; http://www.ccp14.ac.uk/tutorial/lmgp.
(16) Saito, T.; Hayamizu, K.; Yanagisawa, M.; Yamamoto, O.; Wasada, N.; Someno, K.; Kinugasa, S.; Tanabe, K.; Tamura, T.; Hiraishi, J. *Spectral Data Base for Organic Compounds (SDBS)*; http://www.aist.go.jp/RIODB.
(17) *SADABS; Area-Detector Absorption Correction*; Bruker AXS Inc.: Madison, WI, 2004.
(18) *SAINT: Area-Detector Integration Software*, version7.23; Bruker AXS Inc.: Madison, WI, 2004.
(19) Altomare, A.; Burla, M. C.; Camalli, M.; Cascarano, G.; Giacovazzo, G.; Guagliardi, A.; Moliterini, A. G. G.; Polidoro, G.; Spagna, R. *J. Appl. Crystallogr.* **1999**, *32*, 115–119.
(20) Sheldrick, G. M. *SHELXL-97: Program for the Refinement of Crystal Structure*; University of Göttingen: Göttingen, Germany, 1997.
(21) Farrugia, L. J. *J. Appl. Crystallogr.* **1999**, *32*, 837–838.
(22) Merritt, E. A.; Bacon, D. J. *Methods Enzymol.* **1997**, *277*, 505–524.
(23) Macrae, C. F.; Edgington, P. R.; McCabe, P.; Pidcock, E.; Shields, G. P.; Taylor, R.; Towler, M.; van de Streek, J. *J. Appl. Crystallogr.* **2006**, *39*, 453–457.
(24) Nardelli, M. *J. Appl. Crystallogr.* **1995**, *28*, 659.
(25) Diogo, H. P.; Minas da Piedade, M. E. *J. Chem. Thermodyn.* **1995**, *27*, 197–206.
(26) Santos, R. C.; Diogo, H. P.; Minas da Piedade, M. E. *J. Chem. Thermodyn.* **1999**, *31*, 1417–1427.
(27) Pinto, S. S.; Diogo, H. P.; Minas da Piedade, M. E. *J. Chem. Thermodyn.* **2003**, *35*, 177–188.
(28) Kiyobayashi, T.; Minas da Piedade, M. E. *J. Chem. Thermodyn.* **2001**, *33*, 11–21.
(29) Bernardes, C. E. S.; Santos, L. M. N. B. F.; Minas da Piedade, M. E. *Meas. Sci. Technol.* **2006**, *17*, 1405–1408.
(30) Calado, J. C. G.; Dias, A. R.; Minas da Piedade, M. E.; Martinho Simões, J. A. *Rev. Port. Quim.* **1980**, *22*, 53–62.
(31) Diogo, H. P.; Minas da Piedade, M. E.; Fernandes, A. C.; Martinho Simões, J. A.; Ribeiro da Silva, M. A. V.; S., M. M. J. *Thermochim. Acta* **1993**, *228*, 15–22.
(32) Diogo, H. P.; Minas da Piedade, M. E.; Gonçalves, J. M.; Monte, M. J. S.; Ribeiro da Silva, M. A. V. *Eur. J. Inorg. Chem.* **2001**, *228*, 257–262.
(33) Nunes, N.; Martins, F.; Leitão, R. E. *Thermochim. Acta* **2006**, *441*, 27–29.
(34) Marsh, K. N. *Recommended Reference Materials for the Realization of Physicochemical Properties*; IUPAC-Blackwell Scientific Publications: Oxford, U.K., 1987.
(35) Coops, J.; Jessup, R. S.; van Nes, K. In *Experimental Thermochemistry*; Rossini, F. D. Ed.; Interscience: New York, 1956; Vol. 1, Chapter 3.
(36) Nunes, N.; Moreira, L.; Martins, F.; Leitão, R. E. *J. Chem. Thermodyn.* **2007**, *39*, 1201–1205.
(37) Frisch, M. J.; Trucks, G. W.; Schlegel, H. B.; Scuseria, G. E.; Robb, M. A.; Cheeseman, J. R.; Montgomery, J., J. A.; Vreven, T.; Kudin, K. N.; Burant, J. C.; Millam, J. M.; Iyengar, S. S.; Tomasi, J.; Barone, V.; Mennucci, B.; Cossi, M.; Scalmani, G.; Rega, N.; Petersson, G. A.; Nakatsuji, H.; Hada, M.; Ehara, M.; Toyota, K.; Fukuda, R.; Hasegawa, J.; Ishida, M.; Nakajima, T.; Honda, Y.; Kitao, O.; Nakai, H.; Klene, M.; Li, X.; Knox, J. E.; Hratchian, H. P.; Cross, J. B.; Bakken, V.; Adamo, C.; Jaramillo, J.; Gomperts, R.; Stratmann, R. E.; Yazyev, O.; Austin, A. J.; Cammi, R.; Pomelli, C.; Ochterski, J. W.; Ayala, P. Y.; Morokuma, K.; Voth, G. A.; Salvador, P.; Dannenberg, J. J.; Zakrzewski, V. G.; Dapprich, S.; Daniels, A. D.; Strain, M. C.; Farkas, O.; Malick, D. K.; Rabuck, A. D.; Raghavachari, K.; Foresman, J. B.; Ortiz, J. V.; Cui, Q.; Baboul, A. G.; Clifford, S.; Cioslowski, J.; Stefanov, B. B.; Liu, G.; Liashenko, A.; Piskorz, P.; Komaromi, I.; Martin, R. L.; Fox, D. J.; Keith, T.; Al-Laham, M. A.; Peng, C. Y.; Nanayakkara, A.; Challacombe, M.; Gill, P. M. W.; Johnson, B.; Chen, W.; Wong, M. W.; Gonzalez, C.; Pople, J. A. *Gaussian 03*, revision C.03; Gaussian, Inc.: Wallingford, CT, 2004.
(38) Becke, A. D. *J. Chem. Phys.* **1993**, *98*, 5648–5652.
(39) Lee, C.; Yang, W.; Parr, R. G. *Phys. Rev. B* **1988**, *37*, 785–789.
(40) Hariharan, P. C.; Pople, J. A. *Mol. Phys.* **1974**, *27*, 209–214.
(41) Koch, W.; Holthausen, M. C. A. *Chemist's Guide to Density Functional Theory*; 2nd ed.; Wiley-VCH: Weinheim, Germany, 2002.
(42) Spek, A. L. *J. Appl. Cryst. Chem.* **2003**, *36*, 7–13.
(43) Spek, A. L. *PLATON, A Multipurpose Crystallographic Tool*; Utrecht University: Utrecht, The Netherlands, 2007.
(44) Kitaigorodoskii, A. I. *Organic Chemical Crystallography*; Consultants Bureau Enterprises: New York, 1961.
(45) Das, D.; Banerjee, R.; Mondal, R.; Howard, J. A. K.; Boese, R.; Desiraju, G. R. *Chem. Commun.* **2006**, 555–557.
(46) Desiraju, G. R. *CrystEngComm* **2007**, *9*, 91–92.
(47) Anderson, K. M.; Steed, J. W. *CrystEngComm* **2007**, *9*, 328–330.
(48) Nichol, G. S.; Clegg, W. *CrystEngComm* **2007**, *9*, 959–960.
(49) Allen, F. H. *Acta Crystallogr., Sect. B* **2002**, *58*, 380–388.
(50) Babu, N. J.; Nangia, A. *CrystEngComm* **2007**, *11*, 980–983.
(51) Wieser, M. E. *Pure Appl. Chem.* **2006**, *78*, 2051–2066.
(52) Cox, J. D.; Pilcher, G. *Thermochemistry of Organic and Organometallic Compounds*; Academic Press: London, 1970.
(53) Olofsson, G. Assignment of Uncertainties. In *Experimental Chemical Thermodynamics*; Sunner, S., Mansson, M. Eds.; Pergamon Press: Oxford, U.K., 1979; Vol. 1, pp 137–159.
(54) Cox, J. D.; Wagman, D. D.; Medvedev, V. A. *Codata Key Values for Thermodynamics*; Hemisphere: New York, 1989.
(55) Bonino, G. B.; Manzoni-Ansidei, R.; Rolla, M. *Ricerca Sci.* **1937**, *8*, 357–360.
(56) Hubbard, W. N.; Scott, D. W.; Waddington, G. In *Experimental Thermochemistry*; Rossini, F. D. Ed.; Interscience: New York, 1956; Vol. 1, Chapter 5.
(57) Edwards, J. W.; Kington, G. L. *Trans. Faraday Soc.* **1962**, *58*, 1323–1333.
(58) Andrews, J. T. S., Jr.; Bjerrum, N. *J. Organomet. Chem.* **1969**, *17*, 293–302.
(59) Atkins, P. W.; de Paula, J. *Physical Chemistry*, 7th ed.; Oxford University Press: Oxford, U.K., 2002; p 822.
(60) Pascual-Ahuir, J. L.; Silla, E.; Tunon, I. *GEPOL93*.
(61) Bondi, A. *J. Phys. Chem.* **1964**, *68*, 441–451.
(62) Denbigh, K. *The Principles of Chemical Equilibrium*, 4th ed.; Cambridge University Press: Cambridge, U.K., 1981.
(63) Irikura, K. K.; Frurip, D. J. *Computational Thermochemistry. Prediction and Estimation of Molecular Thermodynamics*; ACS Symposium Series No. 677; American Chemical Society: Washington, D.C., 1998.
(64) Computational Chemistry Comparison and Benchmark DataBase. In *NIST Standard Reference Database 101 (Release 12)*; National Institute of Standards and Technology: Gaithersburg, MD, 2005.
(65) Aihara, A. *Bull. Chem. Soc. Jpn.* **1960**, *33*, 194–200.
(66) *Dictionary of Organic Compounds*; Heilbron, D. S. O., Cook, A. H., Bunbury, H. M., Hey, D., Pollock, H. J. R. A., Stevens, R. Eds.; Eyere and Spottiswoode Publishers: London, 1965; Vol. 3.
(67) Chase, M. W. *J. Phys. Chem. Ref. Data* **1998**; NIST-JANAF Thermochemical Tables.
(68) Butland, A. T. D.; Maddison, R. J. *J. Nucl. Mater.* **1973**, *49*, 45–56.
(69) 4-Hydroxyacetophenone BASF Product Bulletin, version 1.0; BASF: Ludwigshafen, Germany, 2003.
(70) Pitzer, K. S.; Gwinn, W. D. *J. Chem. Phys.* **1942**, *10*, 428–440.

CG7012792